AAPS PharmSciTech, Vol. 12, No. 1, March 2011 (© 2011)
DOI: 10.1208/s12249-010-9556-z

Research Article

Solid Dispersions of Imidazolidinedione by PEG and PVP Polymers with Potential Antischistosomal Activities

Francimary L. Guedes,[1,5] Boaz G. de Oliveira,[2] Marcelo Z. Hernandes,[2] Carlos A. De Simone,[3] Francisco J. B. Veiga,[4] Maria do Carmo A. de Lima,[5] Ivan R. Pitta,[5] Suely L. Galdino,[5] and Pedro José Rolim Neto[1,6]

Received 17 May 2010; accepted 30 November 2010; published online 1 March 2011

Abstract. Solid dispersions have been used as a strategy to improve the solubility, dissolution rate, and bioavailability of poor water-soluble drugs. The increase of the dissolution rate presented by (*5Z*)-3-(4-chloro-benzyl)-5-(4-nitro-benzylidene)-imidazolidine-2,4-dione (LPSF/FZ4) from the solid dispersions is related to the existence of intermolecular interactions of hydrogen bond type (>N–H···O<) between the amide group (>N–H) of the LPSF/FZ4 and the ether group (–O–) of the polyethyleneglycol polymer, or the carbonyl (C=O) of the polyvinylpyrrolidone polymer (PVP). The intensity of these interactions is directly reflected in the morphology acquired by LPSF/FZ4 in these systems, where a new solid phase, in the form of amorphous aggregates of irregular size, was identified through scanning electron microscopy and confirmed in the characterizations achieved using X-ray diffraction and thermal analysis of DSC. The solid dispersions with the polymer PVP, in higher concentrations, were revealed to be the best option to be used in the formulations of LPSF/FZ4 in both theoretical and experimental studies.

KEY WORDS: dissolution profiles; imidazolidinedione; polyethyleneglycol; polyvinylpyrrolidone; solid dispersions.

INTRODUCTION

Schistosomiasis is an endemic disease that affects around 74 developing countries. It is found in South America and the Caribbean, Eastern Europe, the Middle East, the Far East, Southeast Asia, and Central and Western Africa. However, more than 80% of those infected by the disease live in sub-Saharan Africa. The drug of choice for treatment of infections caused by all species of *Schistosoma* is praziquantel. Oxamniquine is used in the treatment of infections caused by *Schistosoma mansoni* in some areas where praziquantel is less effective (1).

The imidazolidine nucleus forms part of a broad range of bioactive compounds that also have some schistosomicide properties. Based on this information, various pentagonal heterocyclical imidazolidone derivatives have been synthesized and evaluated for various biological properties, such as (*5Z*)-3-(4-chloro-benzyl)-5-(4-nitro-benzylidene)-imidazolidine-2,4-dione (LPSF/FZ4) which has displayed significant schistosomicide properties *in vitro* (Fig. 1; 2–6). However, this derivative has extremely low water solubility ($S<1$ μg/mL).

The low water solubility of drugs and a low rate of dissolution in gastrointestinal fluids frequently lead to insufficient bioavailability, which is one of the greatest problems faced by pharmaceutical technology. It is estimated that around 35% of commercial drugs and more than 25% of new discoveries present such problems (7).

Various pharmaceutical technologies have been investigated, such as the solid dispersion technique (SD) to improve solubility, the rate of dissolution, and the bioavailability of these drugs.

In solid dispersion, the hydrophilic polymers that have been widely used as carriers are polyvinylpyrrolidone (PVP) and polyethylenoglycol (PEG), owing to their low cost, high solubility in water, and capacity to form dispersions in an amorphous state (8,9).

The aim of this study is to increase the solubility, the rate of dissolution, and the absorption of LPSF/FZ4 by means of solid dispersion using PEG and PVP. The physical–chemical properties of LPSF/FZ4 in these dispersions were characterized using a variety of techniques, including RMN^{1}H spectroscopy, Fourier transform infrared spectroscopy (FTIR), differential scanning calorimetry (DSC), X-ray diffraction (XRD), and scanning electron microscopy (SEM). The study also determined the profile of dissolution of LPSF/FZ4, of the physical mixtures, and the solid

[1] Laboratório de Tecnologia dos Medicamentos, UFPE, Recife, Brazil.
[2] Laboratório de Química Teórica Medicinal, UFPE, Recife, Brazil.
[3] Laboratório de Cristalografia e Modelagem Molecular-LaboCriMM, UFAL, Maceio, Brazil.
[4] Laboratório de Tecnologia Farmacêutica de Faculdade de Farmácia, Universidade de Coimbra, Coimbra, Portugal.
[5] Laboratório de Planejamento e Síntese de Fármacos-LPSF, UFPE, Recife, Brazil.
[6] To whom correspondence should be addressed. (e-mail: pedro.rolim@pq.cnpq.br)

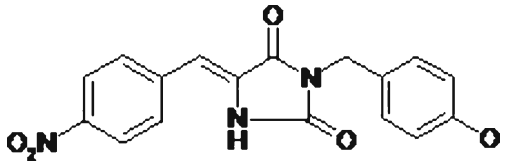

Fig. 1. (5*Z*)-3-(4-chloro-benzyl)-5-(4-nitro-benzylidene)-imidazolidine-2,4-dione (LPSF/FZ4)

dispersions formed with those hydrophilic polymers. The interactions at molecular level of the LPSF/FZ4–polymer complex were evaluated by theoretical calculations involving molecular modeling. Crystallographic data for the compound have been deposited at the Cambridge Crystallographic Data Center as Supplementary Publication No. CCDC 700648.

MATERIALS AND METHODS

Materials

LPSF/FZ4 was designed and synthesized by the Drug Planning and Synthesis Laboratory, UFPE/PE (Brazil), which has a melting point of around 227°C and solubility in water of approximately 0.94±0.03 μg/mL at 25°C. PEG 4000, donated by Oxiteno, Plasdone® K-29/32-type PVP obtained by means of ISP. All the other materials and reagents were of an analytical degree of purity.

Preparation of the Physical Mixtures and SD of LPSF/FZ4 in PEG and PVP

Physical mixtures of the LPSF/FZ4–PEG and LPSF/FZ4–PVP systems containing 20% LPSF/FZ4, carefully weighed (Bioprecisa FA2104N), were prepared in a porcelain mortar, with the aid of a pestle, in accordance with the geometrical dilution method. The mixture was subsequently strained through a 250-μm sieve, placed in an ampoule flask and kept in a dessicator in a vacuum under controlled humidity.

The solid dispersions containing 10%, 20%, and 30% LPSF/FZ4 were prepared using PEG and PVP using the solvent method. Carefully weighed quantities of LPSF/FZ4 and each polymer (Bioprecisa FA2104N) were separately dissolved in methanol/chloroform (1:3 *v*/*v*), and, on dissolving, the solutions were mixed and agitated magnetically for 20 min. The solvent was subsequently removed by evaporation (Fisaton 802) under low pressure (−800±20 mbar) at 40±5°C. The resulting solid dispersions were frozen and liophylized (Liobras L101) for 9 h, strained through a 250-μm sieve, placed in an ampoule flask, and stored in a dessicator in a vacuum under controlled humidity.

In vitro Dissolution

The dissolution profile of LPSF/FZ4 and of the different proportions of complexes formed was carried out in accordance with the specifications of the Food and Drug Administration (FDA) for drugs with poor solubility and the United States Pharmacopeia (USP; 10). Quantities of physical mixture and solid dispersions equivalent to 8 mg of LPSF/FZ4 were carefully weighed and placed in each dissolution vat. The assays were carried out at a temperature of 37±0.5°C, using 900 mL chloridic acid as a buffer solution (pH=1.2) containing 1% of sodium lauryl sulfate, using a two-scoop apparatus rotating at 75 rpm (Varian VK 7010). At fixed intervals of 15 min, for 2 h, samples of 5 mL were taken from the dissolved medium, filtered through 28-μm cellulose filters, and analyzed under UV spectroscopy (B582 Micronal) at 350 nm. Volumes of solvent equal to samples collected were again added to the dissolution vats and, for each binary system, the assays were carried out in triplicate.

The dissolution profiles were evaluated and compared using the parameter of dissolution efficiency in 60 min ($DE_{60\ min}$), calculated on the basis of the area under the dissolution curve of LPSF/FZ4, according to the Khan method (11). The statistical analysis of the $DE_{60\ min}$ was carried out using analysis of variance.

Differential Scanning Calorimetry

The heat characteristics of LPSF/FZ4, of the physical mixture, and of the solid dispersions were analyzed using a Shimadzu DSC-50 System (Shimadzu, Kyoto, Japan). Behavior under heat was studied by heating the samples (2 mg) in an aluminum pan from 25°C to 350°C, a rate of heating of 10°C.min^{-1}, under a flow of nitrogen of 10 cm^3 min^{-1}, using an empty pan as a point of reference.

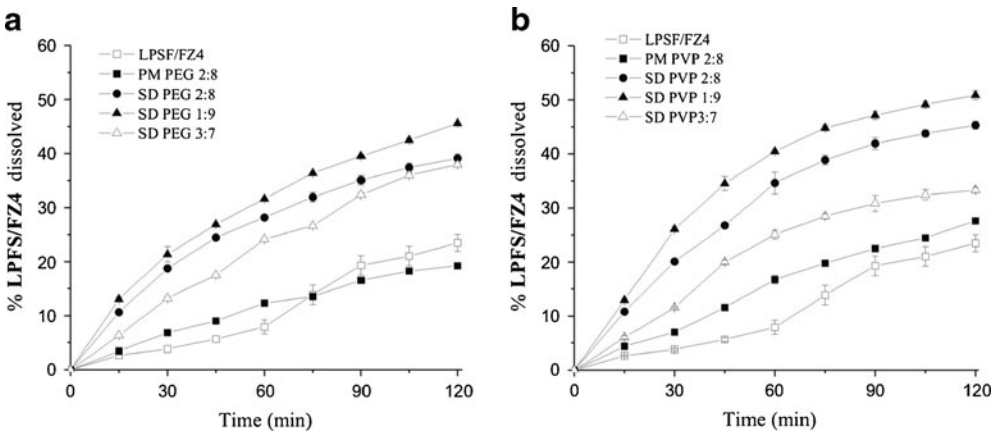

Fig. 2. Dissolution profiles for LPSF/FZ4, physical mixtures, and solid dispersions with PEG (**a**) and PVP (**b**) at stomach acid pH (pH 1.2) containing 1% of sodium lauryl sulfate

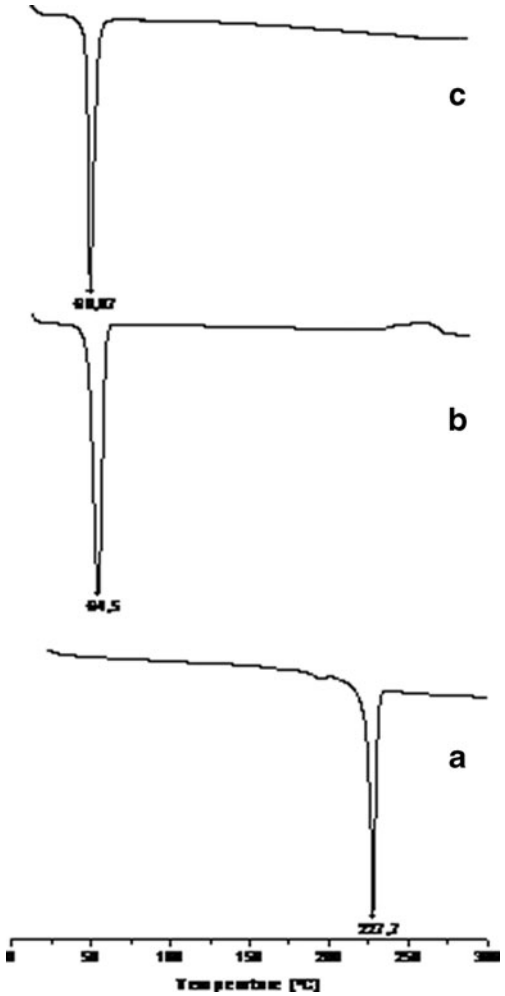

Fig. 3. DSC thermographs for LPSF/FZ4 (**a**), PEG (**b**), and LSF/FZ4–PEG 1:9 solid dispersions (**c**)

Indium (99.98%, melting point 156°C, Aldrich® Chemical Company, Inc., Milwaukee, WI) was used as a standard to calibrate the temperature.

X-ray Diffraction

XRD analyses of LPSF/FZ4 and of the solid dispersions were obtained using a SIEMENS D-5000 diffractometer, equipped with a copper (Cu) anode. The sweep measurements of the 2θ angle were carried out for an interval of 5–50º. The crystallinity of the sample was determined by taking the highest peak of diffraction observed in the solid dispersions as a benchmark. The relation used to calculate the crystallinity was the degree of relative crystallinity (DRC)$=I_{SA}/I_{REF}$, where I_{SA} is the height of the peak of sample under investigation and I_{REF}, the height of the benchmark peak for the same angle, with the highest intensity. The LPSF/FZ4 was used as a benchmark for calculating the DRC values in solid dispersions (12,13).

FTIR

The infrared spectra for the solids dispersed in KBr pellets (containing 1 mg of sample in 150 mg of KBr) were obtained using an IFS 66 Bruker FTIR spectrometer in the 4,000–400 cm^{-1} spectra region, using a resolution of 4 cm^{-1} and a sweep of 100.

Molecular Modeling of FZ4–Polymer Interactions

A previous study with other imidazolidine-2,4-dione system (14) revealed that the following method is appropriate to elucidate the electronic aspects of the intermolecular interactions between the imidazolidine scaffold and the PVP and PEG polymers. The monomers were used instead of the polymers because of the intrinsic difficulty of taking into account all the degrees of freedom for the entire polymer in the quantum chemical calculations employed here. The optimized geometry of the PVP···LPSF/FZ4 and PEG···LPSF/FZ4 hydrogen complexes were obtained using B3LYP/6-31G(d,p) calculations, carried out using the GAUSSIAN 03 program (15). The intermolecular energy values ΔE were determined as $\Delta E = E(\text{complex}) - \Sigma\ [E(\text{isolated molecules})]$, where E(complex) is the energy of the monomer···LPSF/FZ4 complex and E(isolated molecules) refers to the isolated monomer and isolated LPSF/FZ4. These results for intermolecular energy ΔE were traditionally corrected using the zero-point energy (16) and the basis set superposition error (17).

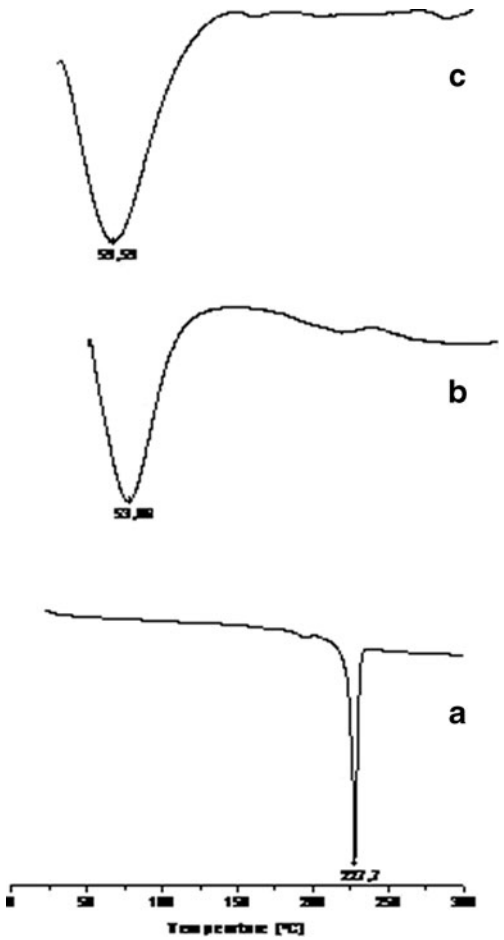

Fig. 4. DSC Thermographs for LPSF/FZ4 (**a**), PVP (**b**), and LSF/FZ4–PVP 1:9 solid dispersions (**c**)

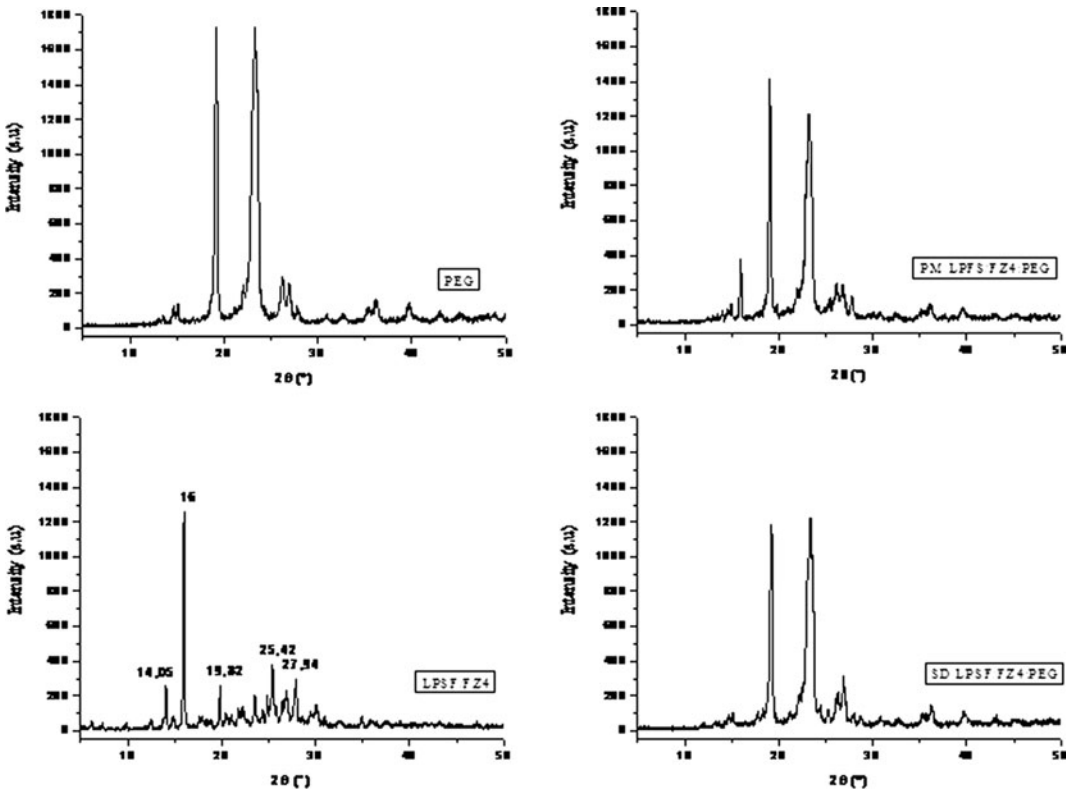

Fig. 5. Diffractographs for LPSF/FZ4, PEG, physical mixture, and LSF/FZ4–PEG 1:9 solid dispersions

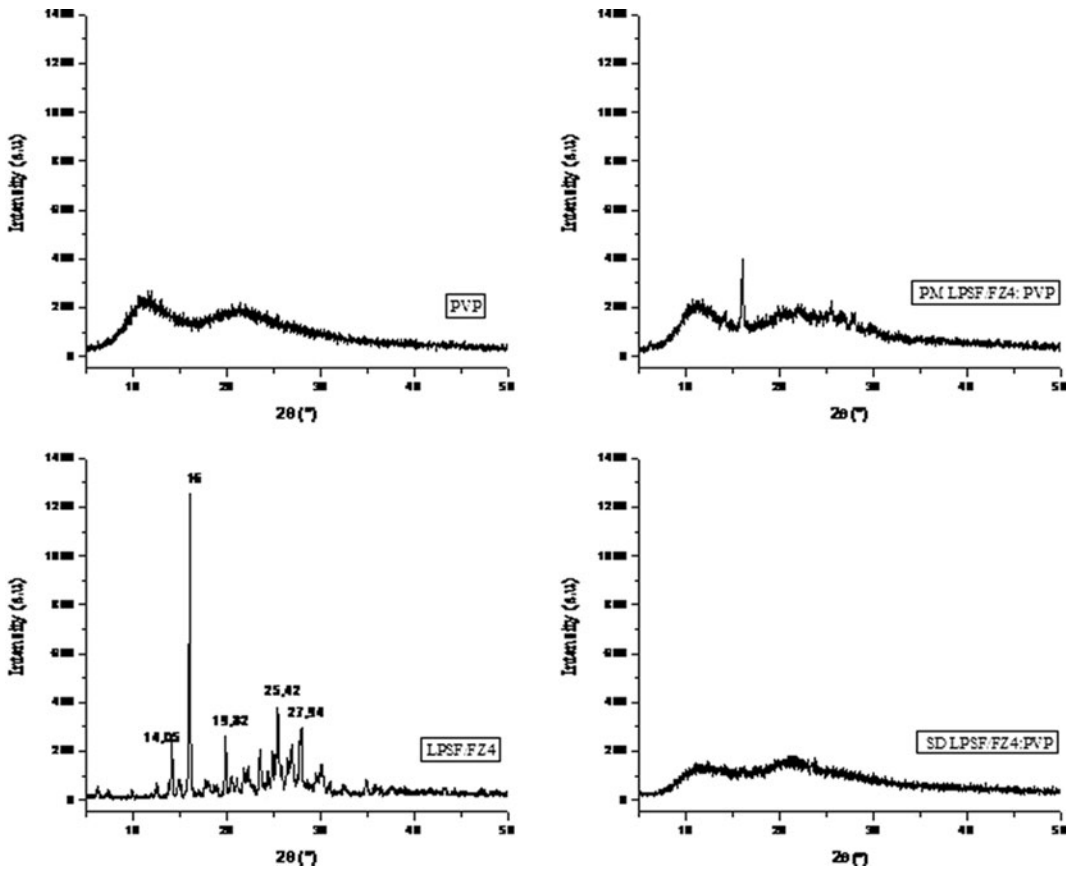

Fig. 6. Diffractographs for LPSF/FZ4, PVP, physical mixture, and LSF/FZ4–PVP 1:9 solid dispersions

Table I. $DE_{60\ min}$ for LPSF/FZ4, Physical Mixtures and Solid Dispersions

	LPSF/FZ4	PM	$SD_{30\%}$	$SD_{20\%}$	$SD_{10\%}$
		LPSF/FZ4–PEG			
$DE_{60\ min}$ (%)	4.02±0,25	6.36±0.10	12.37±0.14	16.97±0.10	19.27±0.40
		LPSF/FZ4–PVP			
$DE_{60\ min}$ (%)	4.02±0.25	7.82±0.16	12.53±0.10	18.74±0.30	23.43±0.43

$DE_{60\ min}$ dissolution efficiency in 60 min, *LPSF/FZ4* (5*Z*)-3-(4-chloro-benzyl)-5-(4-nitro-benzylidene)-imidazolidine-2,4-dione, *PM* physical mixtures, *SD* solid dispersions, *PEG* polyethylenoglycol, *PVP* polyvinylpyrrolidone
All results are expressed as mean±standard deviation

RMN ^{1}H Spectroscopy

The ^{1}H NMR spectra for LPSF/FZ4 and for the solid dispersions were analyzed on Varian Unity Plus 300, using dimethyl sulfoxide (DMSO) as a solvent.

Scanning Electron Microscopy

The morphology of LPSF/FZ4 and its solid dispersions were examined using a Jeol-type SEM (JMS-5600, Japan). The samples were fixed on double-sided carbon adhesive tape, covered in a vacuum with a fine film of gold to make them conduct electricity and were observed at magnitudes ranging from 100 to 4,300.

RESULTS AND DISCUSSION

In vitro Dissolution

The dissolution profile was plotted according to the percentage of LPSF/FZ4 dissolved without becoming complexated and of solid dispersions and physical mixtures against time (Fig. 2).

For evaluation, the DE parameter was calculated in 60 min (Table I). It was shown that the rate of dissolution of non-complexated LPSF/FZ4 was very low (less than 10% at a 1-h interval). Compared with non-complexated LPSF/FZ4, the dissolution of physical mixtures for the two polymers showed a minimal increase, achieving the same percentage dissolution as non-complexated LPSF/FZ4 in a period of 75 min with the PEG polymer. After 75 min, it was observed that the dissolution of non-complexated LPSF/FZ4 exceeded the degree of dissolution attained by the physical mixture LPFS/FZ4–PEG 2:8 (Fig. 2a).

It was seen that an increase in the rate of dissolution of LPSF/FZ4 can be achieved in both solid dispersions (LPSF/FZ4–PEG and LPSF/FZ4–PVP) and the $DE_{60\ min}$ for each system showed a statistically significant difference in comparison with non-complexated LPSF/FZ4 ($P<0.05$).

The dissolution profiles for solid dispersions with PVP in different proportions of LPSF/FZ4–polymer (*p*/*p*), showed a dissolution rate that was somewhat higher, especially in solid dispersions containing 10% LPSF/FZ4 (Fig. 2b). Therefore, the LPSF/FZ4–polymer proportion (10% p/p), in both solid dispersions (PEG and PVP), was selected for continuation of the study.

Differential Scanning Calorimetry

DSC of LPSF/FZ4 displayed an endothermic peak at 227.7°C, the equivalent of its melting point, at the rate of heating used (Figs. 3a and 4a).

PEG is a semi-crystalline polymer and has very low melting point (64.5°C; Fig. 3b). On melting, PEG has the property of being able to dissolve drugs that were complexated prior to attaining their own melting point (7).

This phenomenon may explain the absence of a melting peak for LPSF/FZ4 in the solid dispersions with PEG (Fig. 3c), suggesting that LPSF/FZ4 was completely dissolved in the liquid phase of PEG. Similar results have been reported by other authors (18,19).

PVP is an amorphous polymer (Fig. 4b), and its DSC thermograph in solid dispersions containing 10% LPSF/FZ4 displays a broad endothermic effect ranging from 23.94°C to 135.0°C, with a peak at 59.59°C (Fig. 4c). The disappearance of the peak where LPSF/FZ4 melts suggests that this was no longer present in crystal form and that it had probably assumed a new solid phase with amorphous characteristics in solid dispersions with PVP (17). This may be attributed to the formation of hydrogen bonds between the carbonyl (C=O) group of the PVP polymer and the >NH group of the LPSF/FZ4. Intermolecular interactions with polymers are normally responsible for the disappearance of the crystal melting signal (20).

Table II. DRC for $2\theta=16$ in the LPSF/FZ4–PEG Systems

2θ	LPSF/FZ4	PM LPSF/FZ4–PEG	SD LPSF/FZ4–PEG
16	1,256	375	114
DRC	Ref	0.298	0.09

DRC degree of relative crystallinity, *LPSF/FZ4* (5*Z*)-3-(4-chloro-benzyl)-5-(4-nitro-benzylidene)-imidazolidine-2,4-dione, *PM* physical mixtures, *SD* solid dispersions, *PEG* polyethylenoglycol

Table III. DRC for $2\theta = 16$ in the LPSF/FZ4–PVP Systems

2θ	LPSF/FZ4	PM LPSF/FZ4–PVP	SD LPSF/FZ4–PVP
16	1,256	400	145
DRC	Ref	0.318	0.115

DRC degree of relative crystallinity, *LPSF/FZ4* (*5Z*)-3-(4-chloro-benzyl)-5-(4-nitro-benzylidene)-imidazolidine-2,4-dione, *PM* physical mixtures, *SD* solid dispersions, *PVP* polyvinylpyrrolidone

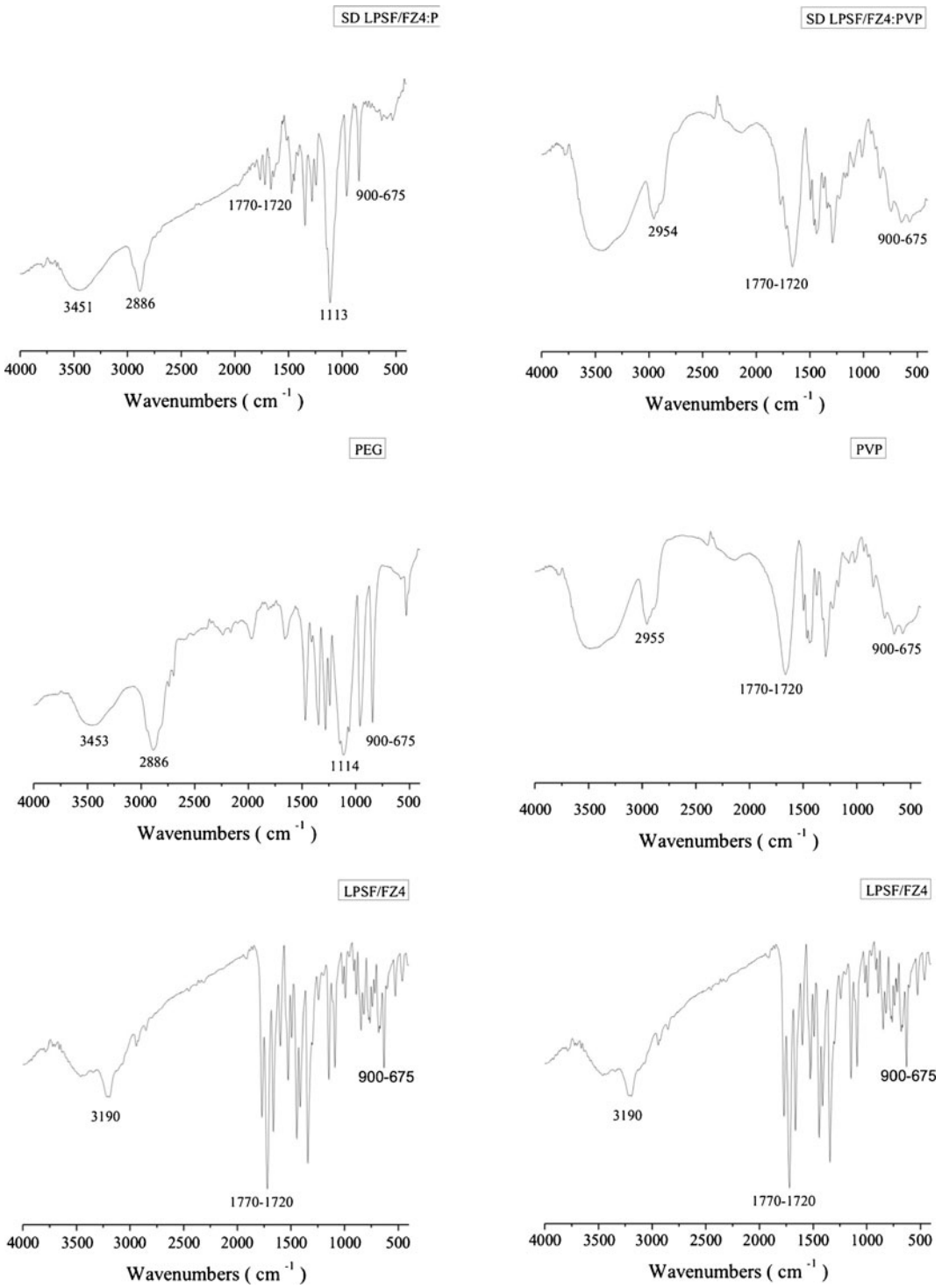

Fig. 7. Infrared Spectra of LPSF/FZ4, PEG, PVP, and solid dispersions

X-ray Diffraction

In the diffractogram for LPSF/FZ4 (Fig. 5), some characteristic peaks in 2θ (angle of diffraction) such as 14.05; 16.0; 19.82; 25.42; and 27.94 are present, revealing the crystalline nature of LPSF/FZ4. The diffraction peak at $2\theta = 16.0$ was used as a point of reference to determine the DRC. X-ray diffraction reveals the physical state of a substance at room temperature. In the physical mixture with PEG, a reduction was observed in the intensity of the benchmark peak for LPFS/FZ4. In solid dispersions with 10% LPSF/FZ4–PEG, the diffractogram revealed that LPSF/FZ4 did not re-crystallize during the preparation of the solid dispersions subsequent to the evaporation of the solvent. There is therefore substantial evidence for the presence of intermolecular interactions between the functional groups of the PEG and of the LPSF/FZ4 in these dispersions. The DRC values for the LPSF/FZ4–PEG system confirm a reduction in the crystallinity of the LPSF/FZ4 of the following order: LPSF/FZ4>MF>DS10% (Table II). It can thus be supposed that LPSF/FZ4 displays a new amorphous solid phase in these solid dispersions or that a significant reduction in the size of particles with low levels of crystallinity has been achieved, these being finely dispersed in the PEG.

In the solid dispersions with PVP, the diffractograph reveals that LPSF/FZ4 is no longer present in its original crystalline form, displaying behavior characteristic of an amorphous substance (Fig. 6). This suggests that the macromolecules of PVP inhibit crystallization of LPSF/FZ4 in solid dispersions. This result accords with the results obtained from the heat analysis (DSC). On the other hand, such behavior was not observed in the physical mixture, where the characteristic LPSF/FZ4 peak can be clearly seen.

In order to obtain the DRC, in this case, only the value of the large diffraction peak was adopted, where it is no longer possible to distinguish the characteristic LPSF/FZ4 peak (21). The values obtained from DRC for the LPSF/FZ4–PVP system confirm the reduction in crystallinity of LPSF/FZ4 of the same order as in PEG (Table III).

FTIR

Other evidence of intermolecular interactions in solid dispersions with LPSF/FZ4–PEG and LPSF/FZ4–PVP were obtained by means of an infrared spectroscopy examination (Fig. 7). The functional groups of LPFS/FZ4 investigated were >NH (3,190 cm^{-1}), C=O (1,770–720 cm^{-1}) and the aromatic groups (900–675 cm^{-1}). The spectrum of the solid dispersions with PEG showed a clear reduction in the C=O band of LPFS/FZ4, angular stretching, and a change to lower –OH band frequencies in the PEG. This may be interpreted as a consequence of the hydrogen bonds between the final –OH groups of the PEG and the C=O of LPFS/FZ4. The infrared spectra of the LPFS/FZ4–PEG and LPFS/FZ4–PVP dispersions suggest the existence of hydrogen bonds between the amide group (>NH) of LPFS/FZ4 and the final –OH or ether (–O–) groups of PEG and the carbonyl (C=O) of PVP. As a result of these interactions, a total disappearance of the amide group (>NH) of LPFS/FZ4 was observed in these systems. The region for the aromatics (900–675 cm^{-1}) of LPFS/FZ4 displayed a marked reduction in intensity, suggesting the presence of van der Waals-type interactions in both solid dispersions. The presence of hydrogen bonds and hydrophobic interactions between LPSF/FZ4 and the hydrophilic polymers in the solid dispersions is the primary cause of the rise in its solubility and dissolution. The basic mechanism is the effect of these interactions on the dimensions of particles and their distribution, as reported in other studies (22–26).

Molecular Modeling of FZ4–Polymer Interactions

According to the results of molecular modeling, the intermolecular energies ΔE calculated for the PEG···LPSF/FZ4 and PVP···LPSF/FZ4 complexes are 20.5 and 41.7 kJ mol^{-1}, respectively, demonstrating the greater stability of the interaction between the LPSF/FZ4 molecule and the PVP monomer. This complex displays twice as much stability as PEG monomer and also has a slightly shorter hydrogen bond (1.80 Å), compared with 1.87 Å for PEG. Figure 8 illustrates the optimized geometries obtained for the PEG···LPSF/FZ4 (I) and PVP···LPSF/FZ4 (II) hydrogen complexes. The strong hydrogen bond established between the imidazolidine and the monomers of PVP and PEG represents the main interaction and justifies this theoretical approach. Besides, other groups (22) are using monomeric models for PVP and PEG to investigate intermolecular interactions with drugs, in a successful way.

RMN ^{1}H Spectroscopy

RMN ^{1}H spectroscopy was used to identify the nature of the interactions occurring between LPSF/FZ4 and PEG or PVP in the 10:90 (*p*/*p*) solid dispersions. $DMSOd_6$ was chosen as an aprotic solvent, since the compounds are soluble in this.

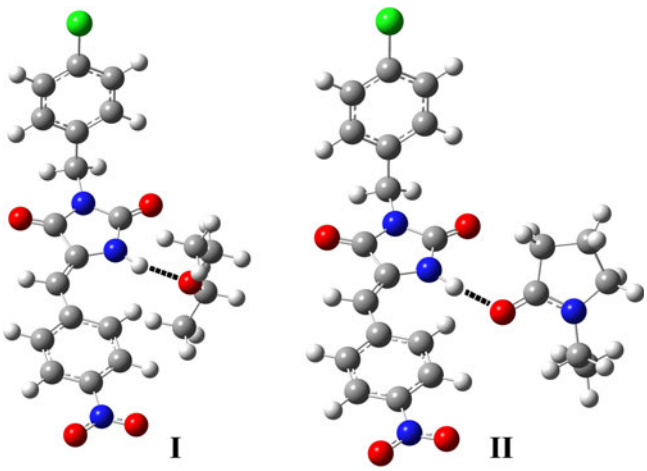

Fig. 8. Optimized geometries obtained for the PEG···LPSF/FZ4 (I) and PVP···LPSF/FZ4 (II) hydrogen complexes, using results of the B3LYP/6-31G(d,p) calculations. The *dashed lines* represent the hydrogen bonds, with 1.87 and 1.80 Å for (I) and (II), respectively. The angles N–H···O between the atoms involved in the hydrogen bonds are 164° and 172°, respectively for (I) and (II)

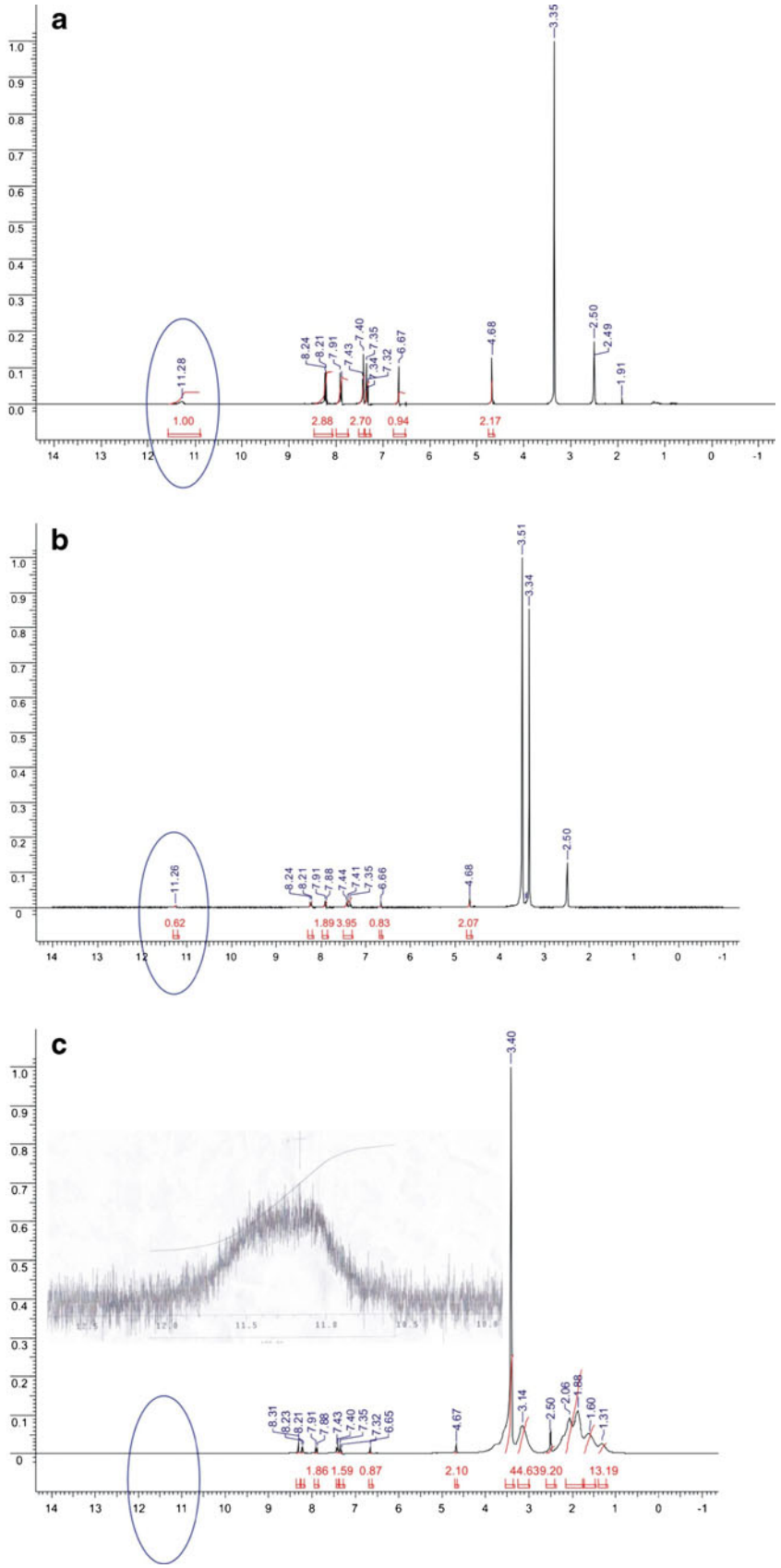

Fig. 9. RMN[1]H Spectra for LPSF/FZ4 (**a**), LPSF/FZ4–PEG solid dispersions (**b**) and LPSF/FZ4–PVP solid dispersions (**c**)

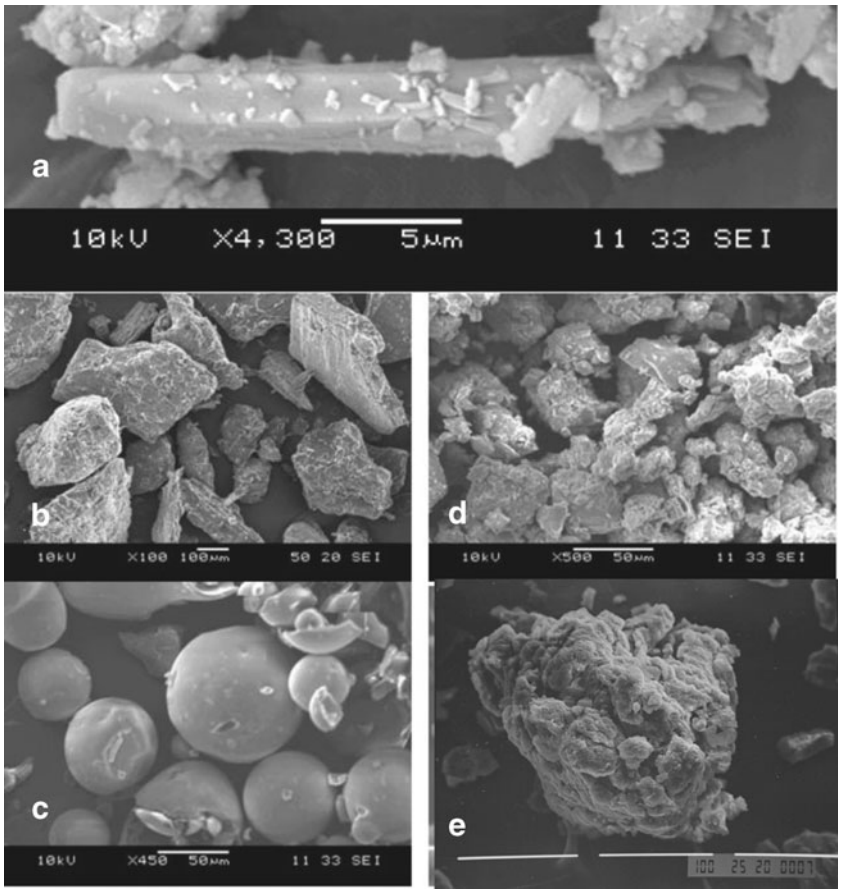

Fig. 10. Electromicrographs for LPSF/FZ4 (**a**), PEG (**b**), PVP (**c**), the LPSF/FZ4–PEG solid dispersions (**d**), and the LPSF/FZ4–PVP solid dispersions (**e**)

Various characteristic peaks can be seen the spectrum for LPSF/FZ4 (Fig. 9a), but this study was mainly concerned to explore and compare the proton that is located in the amide group of LPSF/FZ4, which displays a chemical displacement of 11.28 ppm in the form of a singleton.

In the solid dispersions with PEG containing 10% *p*/*p* of LPSF/FZ4, this peak shows a small change to a lower position of 11.26 ppm, which is not relevant to this study, as it may be related to variations in the equipment itself. However, the reduction observed in the intensity of this peak may indicate the presence of a weak hydrogen bond between the ether group of the PEG and the proton of the amide group of LPSF/FZ4 (Fig. 9b).

In the solid dispersions with PVP containing 10% *p*/*p* of LPSF/FZ4, the peak corresponding to the proton of the amide group at 11.28 ppm was difficult to detect. Magnification of this region revealed that this peak underwent a widening of its bottom line measuring between approximately 11.5 and 11.0 ppm and a significant reduction in intensity (Fig. 9c). This represents a clear indication of the presence of a strong hydrogen bond type intermolecular interaction between the carbonyl (C=O) of PVP and the proton of the >NH amide group of the LPSF/FZ4. These results are in full accordance with those obtained from the study of molecular modeling, and the intensity of these interactions may explain the values obtained from $DE_{60\ min}$ for the dissolution profile.

SEM

The electromicrographs for LPFS/FZ4, PEG, PVP, and the 10:90 (*w*/*w*) solid dispersions are presented in Fig. 10.

LPFS/FZ4 has a needle-shaped crystal morphology (Fig. 10a); PEG is made up of large crystalline particles of irregular size (Fig. 10b), and PVP is composed of spherical particles with some depressions on the surface and amorphous characteristics (Fig. 10c).

In the solid dispersions, the original crystalline morphology of the LPFS/FZ4 has disappeared, and it was not possible to differentiate the morphology of either of the hydrophilic polymers (Fig. 10d, e), in accordance with the results of other authors (27). The electromicrographs for the solid dispersions suggest the presence of a new solid phase, in the form of amorphous aggregates of irregular size, similar to those found by other researchers (23). This behavior is in accordance with the results obtained using heat analysis and X-ray diffraction.

CONCLUSIONS

Many mechanisms have been proposed to explain the increase in solubility and rate of dissolution of drugs in solid dispersions. A reduction in crystallinity, an increase in "wettability", a decrease in particle size, and an amorphous

state are the predominant factors, which are recognized by most researchers in the area.

The partial loss of crystallinity of LPSF/FZ4 exhibited in the solid dispersions may be the result of the weakening of the intermolecular hydrogen bonds present in the crystalline packing of LPSF/FZ4, as shown by preliminary results of a crystallographic study. This weakening is probably related to the establishment of hydrogen bonds involving LPSF/FZ4 and the hydrogen bond acceptor groups of the polymers involved, in accordance with the results obtained using the molecular modeling study (Fig. 8) and the previously applied characterization techniques.

This study confirms that the rise in the rate of dissolution of LPSF/FZ4 in binary solid dispersion systems is directly related to the presence and intensity of intermolecular interactions formed with the hydrophilic polymers, especially the hydrogen bonds identified. These interactions at molecular level appear to control the changes in the physical (crystalline or amorphous) state and to have an influence on particle size.

For the LPSF/FZ4–PVP 1:9 system, which provided better results for dissolution profile, various characterization techniques showed the existence of relatively stronger interactions than those with the PEG polymer, and this was confirmed by the theoretical study of molecular modeling. This suggests that PVP is the preferred polymer for use in formulations developed for LPSF/FZ4 in order to improve its solubility, dissolution, and gastrointestinal absorption.

REFERENCES

1. WHO, Word Health Organization Disease Information, 2001
2. Albuquerque MCPA, Pitta MGR, Irmão JI, Peixoto CA, Malagueño E, Santana JV, *et al*. Tegumental alterations in adult *treated with imidazolidine derivatives. Lat Am J Pharm. 2007;26:65–9.*
3. Pitta IR, Lima MCA, Albuquerque MCPA, Galdino SL. Novel compositions of imidazolidine derivatives useful in the treatment of intestinal schistosomiasis. Braz. Pedido PI, 2005
4. Oliveira SM, Albuquerque MCPA, Pitta MGR, Malagueño E, Santana JV, Lima MCA, *et al*. Behavior of *Schistosoma mansoni* adult worms maintained *in vitro* towards imidazolidinone derivatives. Acta Farm Bonaerense. 2004;23:343–8.
5. Lima MCA, Costa DLB, Goes AJS, Galdino SL, Pitta IR, Luu-Duc C. Synthesis and antimicrobial activity of chlorobenzyl benzylidene imidazolidinediones and thiazolidinediones. Pharmazie. 1992;47:182–4.
6. Galdino SL, Lima MCA, Goes AJS, Pitta IR, Cuong LD. Mass spectrometry of some benzylidene imidazolidinediones and thiazolidinediones. II. Chlorobenzyl imidazolidinedione and fluoro or chlorobenzyl thiazolidinedione compounds. Spectrosc Lett. 1991;24(7–8):1013–21.
7. Bikiaris D, Parageorgiou GZ, Stergiou A, Pavlidou E, Karavas E, Kanaze F, *et al*. Physicochemical studies on solid dispersions of poorly water-soluble drugs evaluation of capabilities and limitations of thermal analysis techniques. Thermochem Acta. 2005;439:58–67.
8. Verheyen S, Blaton N, Kinget R, Mooter GVD. Mechanism of increased dissolution of diazepam and temazepam from polyethylene glycol 6000 solid dispersions. Int J Pharm. 2002;249:45–58.
9. Franco M, Trapani G, Latrofa A, Tullio C, Provenzano MR, Serra M, *et al*. Dissolution properties and anticonvulsant activity of phenytoin-polyethylene glycol 6000 and -polyvinylpyrrolidone K-30 solid dispersions. Int J Pharm. 2001;225:63–73.
10. U.S, Department of Health and Human Services. Guidance for Industry: Dissolution Testing of Immediate Release Solid Oral Dosage Forms, August 1997. Available at: http://www.fda.gov/cder/guidance/1713 bp1.pdf. Accessed on: February 21, 2008.
11. Khan KA. The concept of dissolution efficiency. J Pharm Pharmacol. 1975;27:48–9.
12. Ribeiro L, Loftsson T, Ferreira D, Veiga D. Investigation and physicochemical characterization of vinpocetine-sulfobutyl ether β-cyclodextrins in solid binary and ternary complexes. Chem Pharm Bull. 2003;51:914–22.
13. Veiga MD, Díaz PJ, Ahsan F. Interactions of griseofulvin with cyclodextrins binary systems. J Pharm Sci. 1998;87:891–900.
14. Oliveira BG, Lima MCA, Pita IR, Galdino SL, Hernandes MZ. J Mol Model. 2010;16:119–27.
15. Frisch MJ, Trucks GW, Schlegel HB, Scuseria GE, Robb MA, Cheeseman JR, *et al*. Gaussian 03. Wallingford CT: Gaussian, Inc.; 2004.
16. McQuarrie D. Estatística termodinâmica. New York: Harper & Row; 1973.
17. Boys SB, Bernardi F. Mol Phys. 1970;19:553–66.
18. Mooter GV, Augustijns P, Blaton N, Kinget R. Physico-chemical characterization of solid dispersions of temazepam with polyethylene glycol 6000 and PVP K30. Int J Pharm. 1998;164:67–80.
19. Naima Z, Siro T, Juan-Manuel GD, Chantal C, René C, Jerome D. Interactions between carbamazepine and polyethylene glycol (PEG) 6000: characterisations of the physical, solid dispersed and eutectic mixtures. Eur J Pharm Sci. 2001;12:395–404.
20. Karavas E, Ktistis G, Xenakis A, Georgarakis E. Effect of hydrogen bonding interactions on the release mechanism of felodipine from nanodispersions with polyvinylpyrrolidone. Eur J Pharm Biopharm. 2006;63:103–14.
21. Figueiras A, Carvalho RA, Ribeiro L, Torres-Labandeira JJ, Veiga FJB. Solid-state characterization and dissolution profiles of the inclusion complexes of omeprazole with native and chemically modified β-cyclodextrin. Eur J Pharm Biopharm. 2007;67:531–9.
22. Karavas E, Georgarakis E, Sigalas MP, Avgoustakis K, Bikiaris D. Investigations of the release mechanism of a sparingly water-soluble drug from solid dispersions in hydrophilic carries based on physical state of drug, particle size distribution and drug-polymer interactions. Eur J Pharm Biopharm. 2007;66:334–47.
23. Ruan LP, Yu BY, Fu GM, Zhu D. Improving the solubility of ampelopsin by solid dispersions and inclusion complexes. J Pharm Biopharm Anal. 2005;38:457–64.
24. Sethia S, Squillante E. Solid dispersions of carbamazepine in PVP k30 by conventional solvent evaporation and supercritical methods. Int J Pharm. 2004;272:1–10.
25. Craig DQM. The mechanisms of drug release from solid dispersions in water-soluble polymers. Int J Pharm. 2002;231:131–44.
26. Mura P, Zerrouk N, Mennini N, Moestreli F, Chemtob C. Development and characterization of naproxen–chitosan solid systems with improved drug dissolution properties. Eur J Pharm Sci. 2003;19:67–75.
27. Marzocchi L, Moyano JR, Rossi A, Muñoz P, Arias MJ, Giordano F. Current status of ATPase proton pump inhibitor complexation with cyclodextrins. Biolog J Armenia. 2001;53:176–93.